Defects in Semiconductors - Edited by H. J. von Bardeleben.
Materials Science Forum Volumes 10-12 (1986), pp. 505-514.

APPLICATION OF OPTICALLY DETECTED MAGNETIC RESONANCE TO THE CHARACTERIZATION OF POINT DEFECTS IN SEMICONDUCTORS

J.-M. Spaeth
University of Paderborn, Fachbereich Physik
Warburger Str. 100A, 4790 Paderborn, F.R.G.

ABSTRACT

The observation of optically detected electron spin resonance (ODESR) via donor-acceptor recombination luminescence and via optical absorption is briefly reviewed. Both methods are illustrated with respect to the study of point defects in semiconductors. The present status of the optical detection of electron nuclear double resonance (ODENDOR) is discussed and compared with conventional ENDOR. Possibilities are indicated how ODESR and ODENDOR can be correlated to energy levels and optical properties of defects.

1. INTRODUCTION

Magnetic resonance spectroscopy has proved to be a powerful tool to determine the microscopic structure of paramagnetic point defects. The structure determination is based on the observation of the magnetic interaction between the unpaired electron(s) (or hole(s)) and the magnetic moments of the nuclei in the lattice. If the interaction is observed with the nucleus of a paramagnetic impurity, it is usually called 'hyperfine' (hf) interaction, if it is observed with the nuclear moments of the surrounding lattice nuclei, it is called 'superhyperfine' (shf) or 'Ligand hyperfine' (lhf) interaction /1/. In general the hf interaction is resolved in ESR, which therefore is a useful tool for the chemical identification of impurity defects. The shf interactions are resolved only in few favourable cases. They can usually be resolved by a double resonance technique, in which the nuclear magnetic resonance transitions of nuclei coupled to the unpaired electrons (or holes) are indirectly detected via a change of a partially saturated ESR signal. In this electron nuclear double resonance (ENDOR) technique both hf and shf interactions are measured with a high resolution which is several orders of magnitude higher than in ESR /2,3/. A reliable determination of the microscopic defect structure normally requires ENDOR investigations.

Both ESR and ENDOR can be observed with optical detection. In general, this has definite advantages over the conventional detection: higher sensiti-

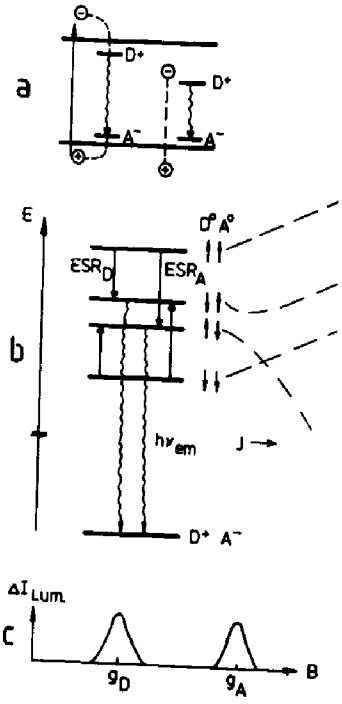

Fig. 1.

a) Schematic energy level diagram for tne excitation and recombination process in a donor-acceptor recombination emission.

b) Energy levels, spin states and the effect of donor-acceptor exchange interaction J of a donor-acceptor pair in a static magnetic field.

c) Optically detected ESR of the donor and acceptor resonances.

vity, high selectivity and the possibility to correlate structural information as contained in the ESR/ENDOR spectra with other defect properties like energy level positions and optical absorption and emission bands. These features have made the optical detection particularly useful in materials research and defect classification. In semiconductors optical detection was so far observed mainly via microwave-induced changes in the donor-acceptor recombination emission /4-7/. Only recently it was also observed via the microwave-induced changes in the magnetic circular dichroism (MCD) of the absorption /8,9/. The latter method was originally developed in color center research in the alkali halides /10-12/.

In this short review both methods will be briefly discussed and compared with respect to their application to the study of point defects in semiconductors. Both methods are also compared to conventional ESR/ENDOR. Finally, possibilities are pointed out to correlate structural information with other defect properties.

2. OPTICALLY DETECTED ELECTRON SPIN RESONANCE (ODESR)

2.1. ODESR via donor-acceptor recombination emission

In crystals containing both donors (D) and acceptors (A) some donors are compensated by acceptors so that both are ionized, D^+ and A^-. We assume a well separated donor-acceptor pair where the separation R is large compared to the radii of the shallow donor and acceptor effective mass states. Above band gap excitation creates electron and hole pairs the electron being trapped at the donor, the hole at the acceptor (see Fig. 1a):

$$D^+ + A^- \xrightarrow{h\nu > E_{gap}} D^0 + \xrightarrow{h\nu_{Emiss}} D^+ + A^- \qquad (2)$$

The energy released as a photon ($h\nu_{Emiss}$) after recombination when the hole on the acceptor fills the electron on the donor is given by

$$h\nu = E_{gap} - E_D - E_A + \frac{e^2}{\epsilon R} \qquad (2)$$

taking into account the Coulomb interaction of charged cores D^+ and A^- in the final state.

The generally accepted mechanism for the observation of ODESR via donor-acceptor recombination is indicated in Fig. 1b, left side, for distant electron hole pair recombination.

The spin exchange interaction between the donor and acceptor is neglected, the hole state is taken as spin only with neglegible contribution from angular momentum. Fig. 1b shows the Zeeman splitting in a static magnetic field. The only selection rule expected to hold is spin conservation ('spin dependent ODESR'). The excitation process occurs via band states and assuming no spin memory in the excitation, all four excited levels are populated with equal rates. The final state after recombination (D^+, A^-) is a spin singlet and due to the selection rule the singlet-singlet recombination has shorter recombination lifetime than the triplet-singlet recombination. In equilibrium the difference in recombination lifetimes will cause an excess of population to build up on the triplet sublevels (spin lattice relaxation time T_1 > recombination lifetime τ). When resonant microwaves are applied the excess population is transferred from the triplet states to the strongly emitting singlet states causing an increase in luminescence intensity. Resonant ODESR signals are observed occurring at magnetic field positions determined by the g-values of the electron and hole centers (see Fig. 1c).

In II-VI semiconductors this technique has been applied with great success, for a review see e.g. /4/. A special problem to be noted is the difficulty to observe the shallow acceptor spectra. From effective mass theory the wavefunctions can be approximated by products of hydrogenic envelope functions and the Bloch functions of the valence band. The top of the valence band is fourfold degenerated and due to a dynamical Jahn Teller interaction each of the four components is mixed with other components by lattice distortion /13/. By applying uniaxial stress the effective strength of the Jahn Teller interaction is reduced and the ESR of the acceptor can be observed.

The spectrometer needed for optical detection via D-A luminescence is comparatively simple, even less complicated than that for conventional ESR. No microwave bridge is needed. The microwave cavity design must allow optical excitation of the sample (often done with lasers) and must contain openings to collect the emitted light. The use of light pipes is advantageous. Conventional ESR spectrometers can be used for ODESR when an 'optical' cavity is used instead of the usual closed cavity. The increase in luminescence intensity is detected at the reference frequency of the chopped microwave using lock-in techniques.

The ODESR observation via emission is the most sensitive way to observe ESR. An estimate of the sensitivity by Geschwind /14/ yielded for the minimum number n_a of spins to be observed

$$n_a = \tau_R / \alpha^2 \eta E \qquad (3)$$

with τ_R the radiative lifetime of the emitting level, α the fractional change in the fluorescence signal induced by the microwave transitions, E the quantum yield of the photon detector and η a geometry factor which contains the details of the setup to collect the emitted light. Taking $\alpha = 0.2$, $\eta = 10^{-3}$, $E = 10^{-2}$ and $\tau_R = 3 \cdot 10^{-3}$s as an example, one obtains $n_a = 3 \cdot 10^4$ spins, independent of the line width. This is to be compared to the sensitivity of conventional ESR, which is $n = 10^{11}$ spins per Gauss line width. The ODESR is certainly several orders of magnitude more sensitive. A fraction of impurities in a surface layer can be observed, which is quite impossible with conventional ESR.

However, the resolution of hf and shf interactions is much worse. The reason is the exchange interaction J between the donor-acceptor pairs. Its influence is indicated schematically on the right side of Fig. 1. If the

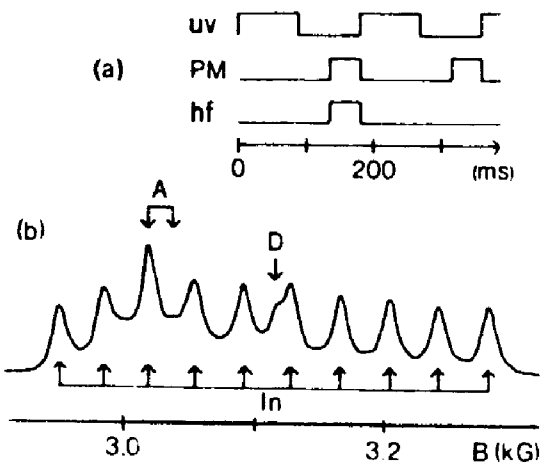

Fig. 2. Time resolved ODESR spectrum of ^{115}In donors in ZnO:Li together with the modulation scheme (UV=laser, hf=microwaves, PM-photomultiplier) lines marked A and D correspond to lithium and gallium resonances, respectively, (from Ref. /7/).

exchange interaction becomes finite the states are mixed and the degeneracy is removed. Different pair separations result in a range of exchange interactions and thus in a broadening of the magnetic resonance line. The only information one gets is that of an averaged g-factor from which alone only little structure information can be gained. A hf resolution can be obtained either from donor-acceptor pairs with a fixed distance like in a donor-acceptor complex or by time resolved ODESR. The latter was demonstrated convincingly for shallow In-donors in ZnO /15/. In the ordinary ODESR spectrum with stationary band-band excitation they could not be detected due to the broadening by exchange interaction. By using pulsed band-band excitation and by observing the microwave-induced change of emission intensity after a delay of 10^{-2} - 10^{-1}s after cutting off the excitation, only distant donor-acceptor pairs were measured. For those the exchange interaction is smaller and correspondingly the radiative lifetime is longer. Fig. 2 shows the result together with the modulation scheme. The 10 line hf structure of ^{115}In donors could now be resolved.

The technique of time resolved ODESR allows a better structure determination, but its disadvantage is the loss in emission intensity. As the resonance effect is only of the order of <1% of the luminescence intensity very often lasers are used to excite the emission, often at excitation energies well above the band gap energy. This is no necessarily advantageous, since due to the high absorption constant only a thin layer of the crystal is excited.

If the photon energy of the excitation light can be changed the luminescence intensity and the ODESR effect can be used to determine the energy level position of donors (E_D) and acceptor (E_A). A recent example for such a type of experiment is that of two phosphorous antisite defects P_{Ga} in p-type GaP:Zn /16/. The emission spectrum of the deep donor P_{Ga} to shallow acceptor Zn luminescence was monitored as a function of the excitation energy with sub-band gap light. The onset of luminescence determines the level position of P_{Ga} relative to the top of the valence band, if the energy level of the acceptor is known.

2.2. ODESR via magnetic circular dichroism of the absorption ('MCD'-method)

The microwave-induced change of the magnetic circular dichroism of both the absorption (MCD) and emission (MCPE) of a defect can be used to measure the ESR of ground and excited states. This was first applied to F-centers in alkali halides /10-12, 17/ but later also to impurity centers like atomic hydrogen in alkali halides /18/ and transition metals in Al_2O_3 /19/. Only recently the MCD technique was applied to III-V semiconductors and shown to be particularly useful /8/. Fig. 3a shows schematically for an atomic s-p-transition (alkali atom) the left (σ^-) and right circular (σ^+) polarised optical transitions in a longitudinal magnetic field (Faraday configuration). The MCD signal measured is

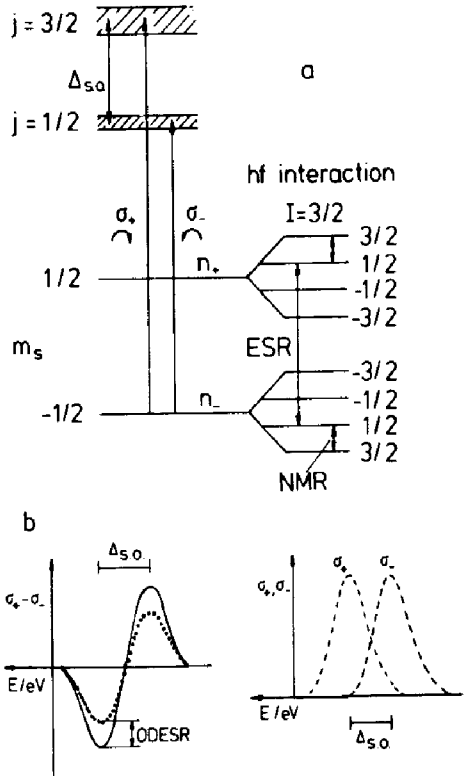

Fig. 3.

a) Simple atomic model to explain the magnetic circular dichroism (MCD) of the absorption and its microwave-induced change to detect ESR and NMR transitions.

b) Rigid shift model for the circular polarised absorptions (σ^+, σ^-) and the resulting MCD line shape ($\sigma^+ - \sigma^-$).

$$MCD = d/4 \quad (I^- - I^+) \tag{4}$$

where d is the sample thickness. I^+ and I^- the intensities for left and right circular polarised light. Circular polarised light is produced by a combination of a linear polariser and stress modulator working at 27 kHz /20/.

In the simple scheme of Fig. 3 the MCD is a derivative structure of a assumed Gaussian phonon broadened absorption band (3b). Its explanation in the so called 'rigid shift' approximation is that the centers of gravity of the σ^+ and σ^- polarised absorption (Fig. 3b) bands shift rigidly in energy by the applied magnetic field without influencing the line shape. For such an MCD its extrema are given by /20/.

$$MCD_{extr.} = \pm \frac{\ln 2}{2e} \frac{\alpha_{max} \cdot d}{W_{1/2}} \cdot \Delta E \tag{5}$$

$$\Delta E = \lambda \cdot \tanh \frac{g\mu_B B_o}{2\,kT} \tag{6}$$

$$\Delta E \quad \alpha \quad \lambda \frac{n_+ - n_-}{n_+ + n_-} \tag{7}$$

where α_{max} is the absorption constant at the peak maximum of the absorption band, $W_{1/2}$ its halfwidth, d sample thickness, λ the spin orbit constant in the excited state, the other symbols have their usual meaning /21/. The spin orbit splitting ($\Delta_{s.o.}$) in the excited state is assumed to be of the same order (or less) than the half width of the phonon broadened absorption band. The $MCD_{extr.}$ is proportional to B and $1/T$, so the favoured experimental conditions are high magnetic fields (1-2 Tesla) and low temperatures (1.4 - 4.2 K). It is given by the occupation difference of the two Zeeman levels (equ. 7). The so called diamagnetic term is omitted in equ. (5) and (6) /20/. The detection of the ESR of the ground state proceeds as follows: by inducing microwave transitions between the Zeeman levels their occupation difference ($n_+ - n_-$) is diminished. This diminuation reduces the value of $MCD_{extr.}$ according to equ. (5), which is monitored. Thus, the ESR is measured as a decrease in $MCD_{extr.}$

The first measurement with this technique in semiconductors was that of the anion antisite (As_{Ga}) defect in semi-insulating GaAs /8/. Although the As_{Ga} contribution to the infrared absorption could not directly be inferred from the absorption spectrum (it is very weak) its paramagnetic MCD of approximately 10^{-3} at 1.5 K and 1 T was clearly observed. The microwave-induced change of that MCD showed the well known 'finger-print' pattern due to ^{75}As hf structure of the As_{Ga} defect. The ODESR effect was surprisingly large about

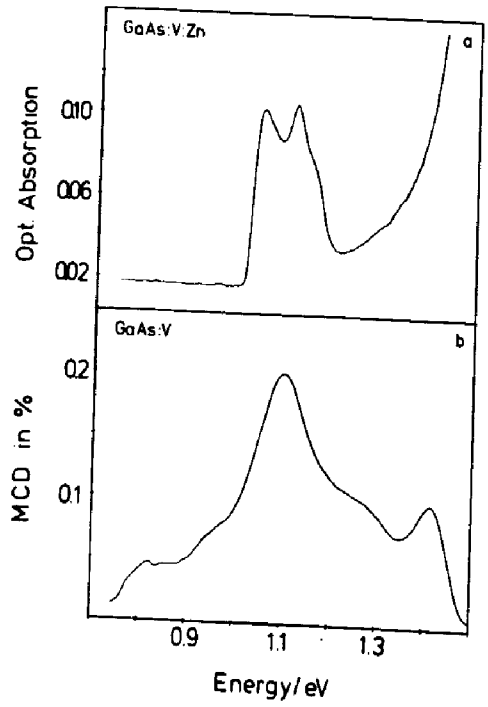

Fig. 4.
a) Optical absorption spectrum of V^{3+} in vanadium doped p-type GaAs:Zn (T = 1.6 K).

b) MCD spectrum in vanadium doped semi-insulating GaAs (T = 1.6 K, H = 2 T).

20% in each of the four ESR lines, the ODESR lines have the same halfwidth as those measured with conventional ESR in 'as-grown' semi-insulating GaAs. The signal to noise ratio was about 2 orders of magnitude higher.

In the case of the As_{Ga} defect the shape of the MCD was interpreted as a superposition of two derivative-like structures due to two intracenter transitions. It must be said, however, that the interpretation of the shape of the MCD constitutes a severe problem especially in semiconductors. Most of the investigations on this problem were made on point defects in alkali halides, where often a detailed knowledge about the atomic ground and excited states is present (transition probabilities, phonon coupling, spin orbit constants).

In semiconductors among intracenter transitions also the photo-ionisation transitions may contribute to the MCD, the strength of phonon coupling and the Franck-Condon shift is often unknown. Therefore, equs. (5-7) should not be taken as a valid description of the effect and the MCD method, except that the MCD is a function of the spin orbit interaction in the excited state and of the ground state spin population.

For the detection of the ESR a better understanding of the MCD line shape is often not really necessary unless one wants to use MCD as a quantitative method to measure absolute defect concentrations (see below). Fig. 4 shows as an example optical absorption and MCD for V^{3+} in GaAs. The absorption spectrum (Fig. 4a) shows the $^3A_2 \rightarrow {}^3T_1(F)$ triple peaked absorption band at 1.1 eV of V^{3+} in p-type GaAs:Zn /22/. In this material the V^{3+} MCD is superimposed by the more than one order of magnitude larger Zn-MCD and no correlation is possible. In semi-insulating GaAs:V on the other hand the As_{Ga} MCD is superimposed, which can, however, persistently be bleached (see Fig. 4b after bleaching). The MCD maximum at 1.1 eV shows similar structure as the absorption, the ODESR spectrum measured at this energy is the same as that measured with conventional ESR and shows the ESR spectrum of V^{3+}. Additional MCD signals around 0.85 eV and 1.0 eV (the zero phonon line of V^{3+} is at 1.008 eV) indicate contributions of photo-ionisation transitions of V^{3+} or possibly transitions originating from V^{2+} charge state.

Without knowledge of the optical cross sections or oscillator strengths and without a quantitative understanding of the optical transitions and the line shape of the MCD, this technique cannot be used to quantitatively determine the defect concentration as can be done in conventional ESR. However, one can estimate the kind of sensitivity one can achieve by using the Smakula formula for the intracenter transitions, including the Lorentz field corrections and assuming a Gaussian absorption band /21/.

$$Nf = 8.7 \cdot 10^{16} cm^{-3} \frac{n}{(h^2+2)} \alpha_{max} W_{1/2} \quad (8)$$

n is the refractive index, N the defect concentration and f the oscillator strength. Inserting equ. (8) and (7) into equ. (5) one obtains

$$MCD_{extr} = 1 \cdot 10^{16} d \cdot N \cdot f \cdot \lambda \cdot \tanh \frac{g\mu_B B_o}{2\,kT} \quad (9)$$

The detection limit for MCD_{extr} is approximately $1 \cdot 10^{-5}$ for a signal to noise ratio of 2:1.

Typical experimental data are: T = 1.4 K, B = 2 T, d = 0.3 cm. Taking as an example the As_{Ga} antisite defects in GaAs one has: n = 3.4, λ = 0.3 eV, $W_{1/2}$ = 0.2 eV, g = 2. This gives $N \cdot f = 10^{11} cm^{-3}$, the minimum concentration of the defects to be detected is $N = 10^{13} cm^{-3}$, independent of the ESR linewidth. In conventional ESR one needs about $10^{16} cm^{-3}$, because of the hf splitting and the large line widths. Thus, the MCD technique is often more sensitive than conventional ESR, the factor being mainly dependent on f and the spin orbit constant in the excited state. As to sensitivity, the ODESR detection via emission is by far superior.

The ODESR of the ground state can be observed in each absorption band which originates from this ground state. This almost trivial statement can be used for a kind of excitation spectroscopy of the ODESR. When monitoring the signal intensity of one particular ODESR line while sweeping the optical wavelength, one obtains only an ODESR signal where an optical transition of the defect is present. Thus, the MCD is 'tagged' by an ESR line, only the MCD belonging to this defect is measured /23/. This is important when the optical absorptions of several defects are superimposed and one needs to determine all optical transitions of one specific defect, as in the case of V^{3+} in semi-insulating GaAs. Fig. 5 shows the 'MCD-tagged by ESR' for the anion antisite defect P_{Ga} in GaP, where several optical transitions into states resonant with the conduction band were discovered in this way /24/.

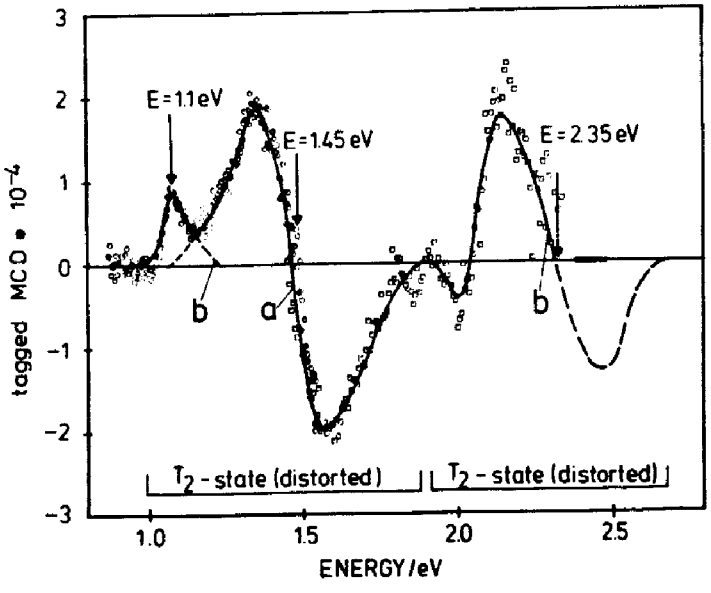

Fig. 5.
MCD spectrum 'tagged by ESR' of the phosphorous antisite defect P_{Ga} in GaP. Optical transitions into excited states resonant with the conduction band are indicated (from ref. /25/).

Of particular importance is the correlation of the ODESR spectra with the energy levels in the gap. This can be achieved in an analogous way as described in section 2.1. by performing photo-MCD and photo-ODESR using a double beam technique. When using p-type material, the energy levels of the deep level defects are not occupied. They can be filled by photo-excitating electrons from the valence band (pumping light) into them and with a second beam (measuring light), then the MCD and the microwave-induced change of the MCD (ODESR) can be measured. The level position is determined by the onset of the MCD signal upon variation of the photon energy of the exciting light. In this way recently the energy levels of the two charge states of As_{Ga}, $As_{Ga}^{++/+}$ and $As_{Ga}^{o/+}$ in GaAs could be determined and with the use of optically detected ENDOR the microscopic structure of a paramagnetic defect can be correlated with its energy levels.

3. OPTICALLY DETECTED ELECTRON NUCLEAR DOUBLE RESONANCE (ODENDOR)

Only very few experiments were reported in semiconductors, where ODENDOR was observed via donor-acceptor recombination emission. There are observations in amorphous silicon /25,26/ and in ZnSe and CdSe /27/. The ENDOR lines were observed as an emission increase upon inducing NMR transitions by a radio frequency applied in a small loop attached to the sample. In ZnSe, for example, 2 lines due to ^{67}Zn and ^{77}Se were seen centered at the frequencies of the free nuclei. The emission enhancement effect was of the order of 1%. The ENDOR lines were broad, about an order of magnitude broader than in conventional ENDOR. The explanation given is that several nuclei contribute to the ENDOR linewidth with different shf interactions, which are not resolved. No angular dependence is reported /27/. Using time resolved techniques, as described in section 2.1., the ENDOR of ^{115}In in ZnO could be observed /15/.

A better way to observe ODENDOR seems to be via the MCD technique. In the level scheme of Fig. 3 the mechanism is qualitatively indicated. In the presence of hf or shf splittings the ESR transitions must obey the selection rule $\Delta m_I = 0$, $\Delta m_S = \pm 1$. Thus, when measuring the ESR in one of the 4 lines of the $I = 3/2$ system, then atmost 1/4 of all spin packets can be involved, only 1/4 of the MCD can be decreased when saturating the transition. However, if each of the 4 lines is inhomogeneously broadened by further shf interactions, then only a fraction of the decrease should occur, since $\Delta m_{I\alpha} = 0$ must be obeyed for the ligands I_α. Thus, upon inducing NMR transitions between the nuclear Zeeman levels one can include more $m_{I\alpha}$ substrates into the ESR pumping cycle and thus increase the effect of decreasing the MCD. Therefore, the ENDOR transitions are detected as a further increase of the ODESR. The first successful experiments of this kind in semiconductors were performed on As_{Ga} defects in GaAs /9/. ENDOR lines of approx. 0.5 MHz width and narrower were observed. They are somewhat broader than usually found in conventional ENDOR. In Fig. 6a part of the conventionally measured ENDOR spectrum of V^{3+} centers in GaAs is shown /28/, in Fig. 6b a section of the ODENDOR spectrum of these defects.

The structural information is obtained from the measurement of the angular dependence of the ENDOR spectra and their analysis with the appropriate spin Hamiltonian. In this an ODENDOR investigation meets the same problems as are found in conventional ENDOR /29,30/. However, the ODENDOR effect was found to be much larger than the conventional ENDOR effect. The latter is of the order of 1% of the ESR effect for typical solid state defect problems. For the As_{Ga} the ODENDOR effect turned out to be of the same order as the ODESR effect, for P_{Ga} defects in GaP about 10% of the ODESR effect. If, however, as in the case of V^{3+} in GaAs the magnetic circular dichroism is small (of the order of 10^{-4}) due to a low oscillator strength or small spin orbit coupling constant the ODESR/ODENDOR spectrum can be measured only with a reasonable signal to noise

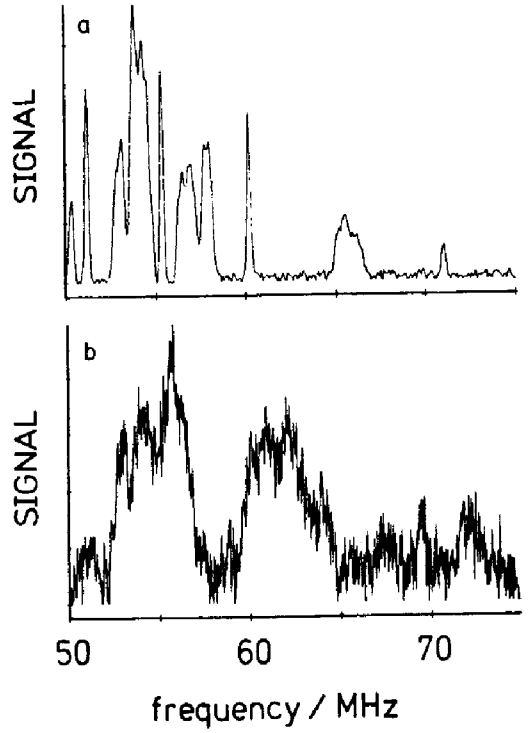

Fig. 6.

Conventionally detected ENDOR spectrum (a) and optically detected ENDOR spectrum of V^{3+} centers in GaAs. (The orientation of the crystal in (b) is not the same as in (a).

ratio using long integration times. The conventional ESR/ENDOR technique, which only monitors the ground state spin polarisation is here favoured (see Fig. 6b).

The experimental setup for the MCD technique is more complicated compared to the emission technique. A cylindrical cavity (mode TE_{011}) is open 360° about the optical axis. For ENDOR 4 rods are introduced close to the sample. They act as 2 rf loops in a Helmholtz arrangement. The sample can be rotated about a vertical axis. The temperature is conveniently held at 1.4 or 1.5 K, below the λ-point of liquid He in order to avoid perturbances of boiling He. It is advantageous to control the temperature accurately, since the MCD effect is proportional to 1/T and microwave and rf powers of about 0.5 W at the sample tend to increase the temperature. The light sources must be very stable to achieve the high MCD sensitivity of 10^{-5}. Therefore, the use of lasers, which have an amplitude ripple of ∿1%, is problematic. For the measurement of ODENDOR at many angles a control of the spectrometer and the data storage by a computer proved to be very useful. Apart from the higher sensitivity compared to conventional ENDOR, the ODENDOR method has the additional advantage of allowing the correlation to optical bands and energy levels in analogy to the experiments described above for the ODESR. Thus, one can measure 'MCD-tagged by ENDOR' as well as photo-ODENDOR, which is a quadrupole resonance experiment. In this way very fine structural details can be correlated with optical properties and energy levels. The power of these possibilities were not yet fully exploited.

References:

/ 1/ Slichter, C.P.: Princ. of Magn. Res., Harper N.Y., 1963
/ 2/ Feher, G.: Phys. Rev., 1959, 114, 1219
/ 3/ Seidel, H.: Z. Physik, 1961, 165, 239
/ 4/ Cavenett, B.C.: Adv. Phys., 1981, 30, 475
/ 5/ Dunstan, D.J. and Davies, J.J.: J. Phys. C, 1979, 12, 2927
/ 6/ Nicholls, J.E., Davies, J.J., Cavenett, B.C., James, J.R. and Dunstan, J.J. J. Phys. C, 1979, 12, 361
/ 7/ Cox, R.T., Block, D., Hervé, A., Picard, R., Santier, C., and Helbig, R.: Solid State Comm., 1978, 25, 77
/ 8/ Meyer, B.K., Spaeth, J.-M. and Scheffler, M.: Phys.Rev.Lett., 1984, 52, 851
/ 9/ Hofmann, D.M., Meyer, B.K., Lohse, F., and Spaeth, J.-M.: Phys.Rev.Lett., 1984, 53, 1187
/10/ Mollenauer, L.F., and Pan S.: Phys. Rev., 1972, B6, 772
/11/ Jaccard, C., Schnegg, P.A., and Aegerter, M.: phys. stat. solg. (b), 1975, 70, 485
/12/ Jaccard, C., and Ecabert, M.: phys. stat. sol. (b), 1978, 87, 497
/13/ Mehran, F., Morgan, T.N., Title, R.S., and Blum, S.E.: J. of Magn. Res., 1972, 6, 620
/14/ Geschwind, S.: Electron Paramagnetic Resonance, S. Geschwind Ed. Plenum N.Y., 1972
/15/ Block, D., Hervé, A., and Cox, R.T.: Phys. Rev. B, 1982, 25, 6049
/16/ Meyer, B.K., Hangleiter, Th., Spaeth, J.-M., Strauch, G., Zell, Th., Winnacker, A., and Bartram R.H.: J. Phys. C: Solid State Phys., 1985, 18, 1503
/17/ Hahn, K., Reyher, H.J., Vetter, Th., and Winnacker, A.: Phys. Lett., 1979, 72, 363
/18/ Meyer, B.K., Heder, G., Lohse, F., and Spaeth, J.-M.: Solid State Comm., 1982, 43, 325
/19/ Geschwind, S, Collins, R.J., and Schawlow, A.L.: Phys. Rev. Lett., 1959, 3, 544
/20/ Henry, C.H., and Slichter, C.P., in: Phys. of Color Centers, Acad. Press N.Y., 1968, Chapt. 6
/21/ Fowler, W.B., in: Phys. of Color Centers, Acad. Press, N.Y., 1968, Chapt.2
/22/ Ulrici, W., Friedland, K., Eaves, L., and Halliday D.P.: phys. stat. sol. (b), 1985, 131, 719
/23/ Ahlers, F.J., Lohse, F., Spaeth, J.-M., and Mollenauer, L.F.: Phys. Rev. B, 1983, 28, 1249
/24/ Meyer, B.K., and Spaeth, J.-M.: Phys. Rev. B, 1985, 32, 1409
/25/ Sano, Y., Morigaki, K., and Hirabayashi, I.: Physica, 1983, 117A, 118B, 923
/26/ Boulitrop, F.: Phys. Rev., 1983, B 28, 6192
/27/ Davies, J.J., Nicholls, J.E., and Barnard, R.P.: J. Phys. C, 1985, C 18, L93
/28/ Hage, J., Niklas, J.R., and Spaeth, J.-M.: J. Electron. Mat., 1985, 14a, 1051
/29/ Seidel, H., Habilitationsschrift, Stuttgart, 1966
/30/ Niklas, J.R., Habilitationsschrift, Paderborn, 1983